DMD Fast Forward. Published on June 21, 2006 as doi:10.1124/dmd.106.010355

On-line Formation, Separation and Estrogen Receptor Affinity Screening of Cytochrome P450-derived Metabolites of Selective Estrogen Receptor Modulators.

S. M. van Liempd, J. Kool, W. M. A. Niessen, D. E. van Elswijk, H. Irth and N. P. E. Vermeulen.

LACDR-Divisions of Molecular Toxicology (S.M.L., J.K., N.P.E.V.) and Biomolecular Analysis (W.M.A.N., H.I.) Vrije Universiteit Amsterdam, The Netherlands and Kiadis B.V. , Groningen, The Netherlands (D.E.E., H.I)

RUNNING TITLE PAGE

Running title

An on-line method for receptor affinity screening of CYP-generated metabolites of SERMs.

Corresponding author

Prof. dr. N.P.E. Vermeulen
LACDR-Section of Molecular Toxicology
Department of Chemistry and Pharmacochemistry
Vrije Universiteit
De Boelelaan 1083, 1081 HV Amsterdam,
The Netherlands

Tel. +31.(0)20.5987590
Fax: +31.(0)20.5987610
email: npe.vermeulen@few.vu.nl

Numbers

Pages	:	35
Words abstract	:	237 (250)
introduction	:	744 (750)
discussion	:	1536 (1500)

Abbreviations

CYPs: Cytochrome P450 enzymes, ERα: Estrogen receptor alpha, HRS: High Resolution Screening, PES: polyethersulphone, RAL: raloxifene, SERMs: selective estrogen receptor modulators, SPE: solid phase extraction, TAM: tamoxifen.

ABSTRACT

We have developed a fully automated bioreactor coupled to an on-line receptor affinity detection system. This analytical system provides detailed information on pharmacologically active metabolites of selective estrogen receptor modulators (SERMs) generated by cytochromes P450 (CYPs). We demonstrated this novel concept by investigating the metabolic activation of tamoxifen (TAM) and raloxifene (RAL) by CYP-containing pig and rat liver microsomes. The high resolution screening (HRS) system is based on the coupling of a CYP-bioreactor to an HPLC-based estrogen receptor alpha (ERα) affinity assay. CYP-derived metabolites of the SERMs were generated in the bioreactor, subsequently on-line trapped with solid phase extraction (SPE) and finally separated with gradient HPLC. Upon elution the metabolites were screened on affinity for ERα with an on-line HRS assay. With this HRS-system, we were able to follow time-dependently the formation of ERα-binding metabolites of tamoxifen and raloxifene. By analyzing the bio-affinity chromatograms with LC-MS/MS structural information of the pharmacologically active metabolites was obtained as well. For tamoxifen, 15 active and 6 non-active metabolites were observed of which 5 were of primary, 10 of secondary and 6 of as yet unknown order of metabolism. Raloxifene was biotransformed in 3 primary and 3 secondary metabolites. Tandem MS/MS analysis revealed that three of the observed active metabolites of raloxifene were not described before. This present automated HRS-system on-line coupled to a CYP-containing bioreactor and an ERα-affinity detector proved very efficient, sensitive and selective in metabolic profiling of SERMs.

INTRODUCTION

The Estrogen Receptor alpha (ERα) plays a crucial role in the development of breast cancer (Ali and Coombes, 2000) and osteoporosis in postmenopausal women (Spelsberg *et al*., 1999). Therefore, selective estrogen receptor modulators (SERMs) are extensively used in treatment and prophylaxis of these disorders. Tamoxifen (TAM) is the most commonly used SERM in the treatment of postmenopausal, hormone sensitive advanced breast cancer. TAM can also halve the threat of breast cancer in women at high risk for this disorder (Morello *et al*., 2002; O'Regan and Jordan, 2002). Raloxifene (RAL) on the other hand is generally used in the prevention of osteoporosis in postmenopausal women. A beneficial effect of the treatment with RAL is that it also reduces the risk of breast cancer (Martino *et al*., 2004). Additionally, RAL has a protective effect on the cardiovascular system by reducing levels of LDL-cholesterol and homocysteine (Morello *et al*., 2002).

It is now well known that most SERMs, like other drugs and xenobiotics are metabolized by membrane bound Cytochrome P450 enzymes (CYPs) (Evans and Relling, 1999; Notley *et al*., 2002). For TAM it has been shown that CYPs in endometrial tissue play a role in the formation of DNA reactive α-hydroxytamoxifen, possibly causing endometrial cancer (Sharma *et al*., 2003). RAL is metabolized by CYPs into three possible quinones with alkylating properties towards macromolecules (Yu *et al*., 2004). Alternatively, both for TAM and RAL it has been shown that their metabolites can also have affinity for ERα (Lim *et al*., 1999; Fura, 2006). Biotransformation of both TAM and RAL is mainly catalyzed by CYP3A4 (Chen *et al*., 2002; Desta *et al*., 2004). Polymorphisms in CYPs or drug-drug interactions at the level of CYPs can cause altered pharmacological effects in humans (Ingelman-Sundberg and Rodriguez-Antona,

2005). Hence, efficient and sensitive screening methods for detection and identification of pharmacologically active metabolites are desirable.

Generation of metabolites and subsequent analysis of metabolite mixtures is usually performed by off-line incubation, extraction and HPLC separation, coupled to various on- or off-line detection techniques. The methods used are usually based on time-consuming manual operations (Roy *et al*., 2005). However, we recently developed and validated a novel bioanalytical system which is based on the hyphenation of a small scale (500 µl) CYP-containing bioreactor to solid phase extraction (SPE) and gradient HPLC (van Liempd *et al*., 2005). This system proved very efficient in the formation, trapping and separation of CYP-generated metabolites. If this method could be combined with a post-column bioaffinity detection system, generated metabolites could be screened instantaneously on selected pharmacological properties. At present, there are several of these so called high resolution screening (HRS) detection systems available. Recently, for example a CYP inhibition and a phosphodiesterase inhibition HRS detection system were developed (Schenk *et al*., 2003; Kool *et al*., 2005). Both methods are based on enzymatic conversion of model substrates in highly fluorescent products. When this reaction is inhibited by substrates or inhibitors, less fluorescent product will be formed and a negative peak in the assay baseline is observed. For the present study we made use of an HRS assay for the detection of ERα-binding compounds (Oosterkamp *et al.*, 1996; Schobel *et al.*, 2001; Kool *et al.*, 2006). This HRS bioaffinity assay is based on the increase of fluorescent signal of the tracer compound coumestrol upon binding to the ERα ligand binding domain. When coumestrol is displaced by a compound with ERα-affinity that elutes from the HPLC column, it is seen as a negative peak in the base line of the bioassay.

The objective of the present study was the development of a hyphenated and automated HRS system that provides information about the time-dependent formation and the ERα-affinity of on-line generated metabolites of SERMs. Metabolites were generated in an adapted version of a recently developed on-line CYP bioreactor, coupled to SPE and gradient HPLC (van Liempd *et al*., 2005). For the biotransformation of TAM, easily available CYP-containing pig liver microsomes were used. Especially CYP1A2, CYP3A4 and CYP2E1 activities of these microsomes show great resemblance to those in human liver (Zuber *et al*., 2002). For the biotransformation of RAL, phenobarbital (PB) induced rat liver microsomes were used, because they contain high levels of CYP2A and 3A subtypes (Gokhale *et al*., 1997). By coupling the CYP bioreactor to an HRS ERα affinity detection system, it is possible to screen the on-line metabolites for ERα-affinity in a post column detection mode. By analyzing the detected active metabolites with LC-MS/MS structural features of these metabolites could be resolved.

EXPERIMENTAL SECTION

Materials. Tamoxifen (TAM), raloxifene (RAL), phenobarbital (PB), Glucose-6-phospate (G6P) and Glucose-6-phosphate dehydrogenase (GDH) were obtained from Sigma-Aldrich (Zwijndrecht, The Netherlands). Riedel de Häen (Seelze, Germany) supplied sodium hydroxide, sodium chloride, magnesium chloride, potassium dihydrogenphosphate, dipotassium hydrogenphosphate, sodium thiosulphate, acetic acid (AA), HPLC grade methanol and ammonium acetate. β-Nicotinamide adenine dinucleotide phosphate (NADPH) tetra sodium salt and ethylenediaminetetraacetic acid (EDTA) were purchased from Applichem (Lokeren,

Belgium). Bovine serum albumin (BSA) was obtained from Gibco/BRL (Breda, The Netherlands).

Biomaterials. CYP reaction buffer consisted of 100 mM potassium phosphate (pH=7.4), 10 mM $MgCl_2$, 16.0 mg/ml BSA and 2 mM EDTA. The buffer used in the HRS ERα-affinity assay consisted of 10 mM KP_i (pH=7.4) and 150 mM NaCl (EB). The regenerating system (RS) for the CYP reaction contained 10 mM NADPH, 30 mM G6P and 3 u/ml GDH dissolved in CYP reaction buffer. TAM and RAL were dissolved in 0.1% AA upon injection. Pig liver microsomes (LMs) were prepared as described by Kool *et al.* (Kool *et al.*, 2006) and contained 20 μM CYP as determined according to Sato *et al*.(Omura and Sato, 1964) PB induced rat LMs were prepared according to Yenes *et al* (Yenes *et al*., 2004) and contained 11 μM CYP. The ERα ligand binding domain (LBD) was produced with recombinant E. coli BL21(DE3)-expressing His6-ER_LBD according to Eiler *et al* (Eiler *et al*., 2001). The concentration of ERα_LBD was measured by determination of estradiol binding ability in a saturation radioligand binding assay described by Eiler *et al* (Eiler *et al*., 2001) and yielded 250 nM.

SPE-HPLC-coupled CYP Bioreactor. Formation and separation of metabolites took place in a slightly modified model (Fig. 1) of a recently developed and validated on-line bioreactor, coupled to SPE and HPLC (van Liempd *et al*., 2005). All pumps used in the system were Knauer K-500 HPLC pumps. Injections were performed with a Gilson 234 autoinjector (50 μl injection loop) equipped with a Rheodyne 6-port injection valve. Autoinjector, pumps and switch valves were operated by ScreenControl software (Kiadis, Groningen, The Netherlands). The HPLC columns, SPE columns and reaction coils were thermostated with a Shimadzu CTO-10AC column oven. Superloops were purchased from GE Healthcare (Roosendaal, The Netherlands). Knitted 1/16" × 0.75mm PTFE reaction coils, PEEK tubing, 6-way dead-end switch valves and 2-position 6-port

switch valves were obtained from VICI Jour (Amstelveen, The Netherlands). Flow splitters were made of 1/16" × 0.5 mm PEEK tubing with 50 µm I.D. × 375 µm O.D. fused silica inserts. Polyethersulphone (PES) 0.22µm membrane filters were purchased from Sterlitech (Kent, WA, USA). The filter was embedded between PEEK inserts with pore size of 150 µm in order to fixate the flexible PES membrane. Filter and inserts were enclosed by a PEEK filter holder, described in a preceding publication (van Liempd *et al.*, 2005). The inserts and filter holder were manufactured in house. SPE cartridges were prepared in house. A slurry of 100 mg/ml SPE materal in MeOH was prepared. SPE materials used were Luna C18(2) 10 µm (Bester, Amstelveen, The Netherlands), StrataX (Bester, Amstelveen, The Netherlands) and C8 Bakerbond (J.T Baker, Deventer, The Netherlands). The slurry was transferred in a 10 × 3 mm column by applying underpressure at the end of the column. The bottom was sealed with a 0.2 µm stainless steel screen. When the column was filled, the top was sealed with a similar screen.

Optimization of the CYP Bioreactor. Since different substrates were used in this bioreactor set-up when compared to the one previously developed (van Liempd *et al.*, 2005), the reactor had to be revalidated. First, absorption of the RAL and TAM to flow path components (tubing, reaction coil, filter unit) was evaluated. Therefore, the filter outlet was directly coupled to the UV detector. Next, the substrate (50 µl, 500 µM) or control was injected and mixed with CYP reaction buffer (without microsomes) in the reaction coil. The flow path was then emptied through the UV detector with water or with 0.1 % (v/v) acetic acid. The obtained signals were subtracted from controls and compared to the signal obtained by direct injection of substrates in the detector. Subsequently, properties of various SPE materials were assessed. SPE materials were tested on breakthrough volumes with a method previously described (van Liempd *et al.*, 2005). During separation the SPE column is placed in series with the HPLC column, therefore the

effect of the SPE material on separation had to be determined. For this purpose, peak widths of substrate peaks were compared for different SPE materials, i.e Strata-X, Luna C18(2) 10 µm and C8 Bakerbond.

On-line Metabolite Formation and Separation. The SPE-HPLC-coupled CYP bioreactor can be divided in a CYP reactor unit and a chromatographic unit (Fig. 1). In the bioreactor unit the actual CYP reaction takes place while in the chromatographic unit analytes are trapped and separated. For the present study, we applied a few alterations in both the bioreactor and the chromatographic unit. For the reactor unit this included incorporation of three extra reaction coils with accompanying switch valve (SV2). Additionally, in the chromatographic unit three extra SPE cartridges, a switch valve (SV5) and an SPE wash pump (P4) were introduced.

In more detail, the bioreactor unit consisted of a pump (P1), switch valves (SV1-SV3), an autoinjector, reaction coils, a filter unit and 50 ml superloops. A Superloop (SL) is a hydraulic driven syringe that can introduce various solutions in the system. SL 1 was filled with CYP containing microsomes and SL 2 contained regenerating system (RS). Both SL 1 and 2 were kept on ice. During filling of the reaction coil, the flow of P1 was split between the autoinjector, SL 1 and SL 2 in a 1:8:1 ratio. Control runs were carried out by blocking the RS flow by means of a manual operated switch valve (not indicated in fig. 1) between SL 3 and the 7-way junction. The total reaction volume amounted 500 µl. Following incubation, analytes were applied to the SPE column with a degassed 0.1% AA solution from SL 4. All parts in the reactor unit were connected with 1/16" × 0.5 mm I.D. PEEK tubing.

The bioreactor and the chromatographic unit were separated by a filter unit containing a 0.22 µm polyethersulfone (PES) filter in order to remove microsomes that otherwise could clog the SPE and HPLC columns. After reconcentration of analytes on the SPE column the filter unit and

reaction coil were rinsed by a series of cleaning steps. First, the filter was back flushed with water at a flow rate of 1 ml/min for 1 min followed by a solution of 250 mM NaOH/0.5% SDS (SL 4) at the same flow rate for 1 min. Finally, the system was rinsed with water at a rate of 1 ml/min for 3 min which proved to be sufficient for total removal of the washing solution (pH went back to 7).

Chromatography. Prior to HPLC separation, the SPE column, containing Luna C18(2) 10 µm particles, was washed with 2 ml of a 5% MeOH solution. Next, the compounds were separated in the chromatographic unit, which consist of gradient pumps (P2, P3), an SPE wash pump (P4), switch valves (SV4, SV5), SPE columns and an HPLC column. For TAM and its CYP generated metabolites a linear gradient from 50% MeOH to 90% MeOH in 40 min, constant for 20 minutes and back to 30% MeOH in 10 min was applied. RAL and its metabolites were separated with a gradient from 30% MeOH to 80% MeOH in 40 min, constant for 20 min and back to 30% MeOH in 10 min. For both gradients, organic and aqueous phases contained 10 mM ammonium acetate. All separations were carried out on a 150 × 4.6 mm I.D. Luna C18(2) column protected with a 2.0 × 5.0 mm I.D. C18 guard column (Phenomenex, Amstelveen, The Netherlands). The HPLC flow rate for all separations was 250 µl/min. After the HPLC column, the eluent was split in a 9 to 1 ratio to respectively a Agilent 1100 series UV detector (Agilent Technologies, Amstelveen, The Netherlands) and the on-line ERα affinity assay. The UV detector was set to 280 nm when TAM was used as a substrate and to 254 nm when RAL was used. HPLC column and SPE cartridges were thermostated at 37°C and 22°C respectively. All parts in the chromatographic unit were connected with 1/16" × 0.13 mm I.D. PEEK tubing.

Reaction Conditions. For one reaction procedure with one control run and three reaction runs, the first coil (**a**) was filled only with microsomes and substrate (TAM or RAL) at a flow rate of

0.5 ml/min (table 1). The other coils (**b-d**) were filled with microsomes, substrate and RS. The final coil concentrations in the reaction runs with TAM were 50 μM TAM, 1.6 % (v/v) pig LMs (360 nM), 1.0 mM NADPH, 3.0 mM G6P and 0.3 u/ml GDH in a total volume of 500μl. Coil concentrations for RAL incubations were 25 μM RAL and 8% (v/v) rat LMs (880 nM) whereas all the other components were kept the same as in TAM incubations. Reaction coils were thermostated at 37°C. Next, the coils were emptied one after another, starting with **d** ending with **a**. The mixture in the reaction coils was applied to corresponding SPE columns (e.g coil **a** to SPE column **a**) with 0.1% (v/v) AA from SL 4 at a flow rate of 1.0 ml/min. The injection and coil emptying procedures were programmed such that incubation times in the different coils were 7, 15 and 24 min. When all coils were emptied on SPE columns, the trapped compounds were further separated on an HPLC column.

HPLC and Mass Spectrometry. To identify metabolites, reaction or control mixtures were trapped on the SPE columns as described. Subsequently, the SPE columns were transferred to the LC-MS/MS setup and placed in front of the HPLC column. The same gradients were used as in the on-line ERα affinity assay. For both TAM and RAL MS was performed on an LCQ Deca mass spectrometer (Thermo Finnigan, Breda, The Netherlands) in full scan (*m/z* 100-800) and positive electrospray ionization (ESI) mode. The most abundant ion was selected for collision-induced dissociation (CID). Eluent from the HPLC column was sprayed into the mass spectrometer at +4.5 kV. The temperature of the heated capillary was set at 240 °C; sheath and auxiliary gas flows were 10 and 50, respectively. An UV detector was placed in series with the MS. By aligning UV spectra obtained with the bioassay setup and those obtained prior to MS, masses could be appointed to compounds, responsible to ERα-affinity signals.

Estrogen Receptor Alpha Affinity Assay. The present homogenous ERα-affinity detection assay was performed according to Kool *et al* (Kool *et al.*, 2006). The ERα-affinity detection system is based on the competition of a fluorescent tracer compound (coumestrol) with HPLC-eluted compounds for the ligand-binding domain of ERα (LBD). When coumestrol is bound to the receptor, fluorescence is enhanced. When binding of coumestrol is decreased due to competition of an eluting ERα ligand, fluorescence intensity decreases. This decrease is a measure of affinity of the ligand towards ERα. A setup was used that consisted of make up pumps (P5, P6), superloops (SL 5, 6), reaction coils (1/16" × 0.25 mm I.D., Tefzel) and a Agilent 1100 series fluorescence detector (Agilent Technologies, Amstelveen, The Netherlands) (Fig. 2). The HPLC eluent was split in a 1:10 ratio where one tenth of the flow (25µl/min) was directed to the assay. In the 4-way junction, this flow was combined with the ERα solution (10 nM ERα in EB, SL 5) flow of 150 µl/min and a make up flow. One tenth of the total make up flow was directed to the assay (135 µl/min). The make up flow consisted of an opposite H_2O/MeOH gradient compared to the HPLC gradient in order to keep the MeOH concentration in the assay constant at 15%. ERα and eluted compounds were allowed to bind in the first reaction coil (25 µl). This mixture was combined with the flow of coumestrol solution (0.43 µM in EB, SL 6) of 150µl/min. The final equilibrium between ERα, ligand and coumestrol was established in the second reaction coil (50 µl). Detection took place directly after the second coil with a fluorescent detector set to λ_{ex} = 340 nm and λ_{em} = 410 nm.

Data analysis. For both substrates, three consecutive reaction procedures including HPLC separation and on-line ERα affinity screening were performed in order to measure metabolite formation in time. Areas of negative peaks in the baselines of the ERα affinity assay, caused by eluted, active metabolites and corresponding UV traces were integrated with ACD/SpecManager

6.0 (Advanced Chemistry Development Inc., Toronto, Canada). A threshold of S/N > 3 was applied for appointing negative peaks. For obtaining the relative ERα affinity, all integrated areas of all ERα-affinity traces were expressed as a percentage of the largest area (parent compound excluded). Relative affinities of corresponding signals were averaged and relative standard deviations (RSD) were calculated with Prism 3.0 (GraphPath Software inc, San Diego, CA). Deviations of ERα-affinity signals after 24 min incubations from controls were checked on significance with a two-tailed t-test. LC–MS data of the metabolites were processed with Xcalibur/Qual Browser v 1.2 (Thermo Finnigan).

RESULTS

We have developed a new and fully automated, on-line system, which is able to metabolize two representative SERMs with CYP enzymes and to screen the metabolites formed for ERα-affinity. To that end, two recently developed and validated methodologies i.e., an on-line bioreactor (van Liempd *et al*., 2005) (Fig. 1) and an on-line ERα-affinity bioassay (Oosterkamp *et al*., 1996) (Fig. 2), were combined into one hyphenated system. The metabolites generated in the multi-coil CYP-bioreactor could be trapped on-line with a SPE unit and separated with gradient HPLC. Subsequently, the separated metabolites were screened for ERα-affinity with the on-line ERα-affinity bioassay. Overall, this approach resulted in the generation and detection of 15 ERα-binding and 6 non-binding metabolites for TAM (Fig. 3). Moreover, the multi-coil CYP-containing bioreactor was able to produce metabolites of RAL or TAM in a time-dependent way (Fig. 5). For RAL, 6 binding and two non-binding metabolites were detected (Fig. 4). The concentration of all metabolites of both TAM and RAL increased in time except for metabolites TM6 and TM 15, which decreased after 7 min incubation. The *m/z* values of most metabolites formed could be determined by analyzing the SPE trapped compounds with mass spectrometry. For identification, subsequent MS-MS spectra provided further information about the structure of the metabolites (see below).

Optimization of the analytical method. In the present bioreactor set-up, the liver microsomal incubations took place prior to the corresponding HPLC runs instead of after each HPLC run. As a consequence, we were able to decrease the total run time with 10% compared to the previous bioreactor set-up (van Liempd *et al*., 2005) where HPLC gradients of 70 min were applied. The newly developed bioreactor system with multiple reaction coils and multiple SPE units was

DMD Fast Forward. Published on June 21, 2006 as DOI: 10.1124/dmd.106.010355
This article has not been copyedited and formatted. The final version may differ from this version.

optimized for two SERM substrates. To that end, we tried to diminish adsorption of substrates and metabolites to flow path components of the bioreactor and the SPE unit as much as possible. Flow path flushing with MilliQ water only resulted in a recovery of 75% for both TAM as RAL, while flushing with 0.1 % (v/v) acetic acid resulted in a recovery of >99% of both substrates (data not shown). During reaction coil flushing in the presence of liver microsomes, the pressure over the filter increased from 0 to 10 bars when a 2% (v/v) pig LM solution was used and from 0 to 20 bars when a 10% (v/v) rat LMs solution was used. When the filter membrane was cleaned with MilliQ water and NaOH/SDS solution the pressure returned to normal. Evaluation of SPE materials showed that all materials tested, i.e. Luna C18(2), C8 Bakerbond and Strata-X, were able to trap both TAM and RAL (50 µl, 500µM) and could trap both substrates completely. However, only Luna C18(2) 10 µm material did not alter peak widths during HPLC separation when compared to the same separation without SPE column. The use of other SPE materials resulted in wider peaks for TAM and RAL, i.e. 1.6 times for Strata-X and 1.9 times for C8 Bakerbond.

After the optimization, the SPE-HPLC combination coupled to the CYP-bioreactor could be used for the metabolic conversion of the two substrates. This resulted in the generation of 21 metabolites of TAM and 7 for RAL. Besides the unchanged substrates, many metabolites with affinity for ERα were eluting from the HPLC column and causing negative peaks in the baseline of the ERα-affinity trace (Fig. 3B and 4B). Tamoxifen was metabolized by pig LMs in 15 ERα-binding metabolites (TM1-TM15, Fig. 3) and 6 non-ERα-binding metabolites (TM16-TM20). Relative ERα-affinity progress curves showed that the formation of ERα-binding metabolites was time dependent (Fig. 5). We arbitrarily distinguished ERα-binding metabolites in highly active (TM6, TM8, TM11, TM12, TM13, Fig. 5A), moderately active (TM5, TM9, TM10,

DMD Fast Forward. Published on June 21, 2006 as DOI: 10.1124/dmd.106.010355
This article has not been copyedited and formatted. The final version may differ from this version.

TM14, Fig. 5B) and low active metabolites (TM1-TM4, TM7, TM15, Fig. 5C) according to their relative affinity for ERα after 24 min of incubation in the bioreactor. Relative ERα-affinities for the strong binding metabolites varied from 97 ± 5% for TM11 to 15 ± 4% for TM12. The 4 moderately active metabolites showed affinities varying from 8.4 ± 1.4% to 5.6 ± 3.0%. The low active metabolites possessed activities from 4.0 ± 1.2% to as little as 1.6 ± 0.9%. When the five TAM metabolites with high relative ERα-affinities were taken into account the total relative standard deviation (RSD) of the data points amounted 28%. For metabolites with moderate ERα-affinity, a RSD of 37% was calculated while for slightly active metabolites the RSD was 43%. After 24 min of incubation of TAM with pig LMs, all active metabolites showed a significant rise in activity compared to control incubations ($p<0.05$). Moreover, from the relative ERα-affinity progress curves (Fig. 5) upward trends of ERα-affinity in time, indicative of increasing production of active metabolites, were obvious. Biotransformation of RAL by rat LMs resulted in the formation of 6 active metabolites (RM1-RM6) and one none-active metabolite (RM7) (Fig. 3B). The pooled RSD of all six active RAL metabolites was 18%. Again, upward trends in the formation of ERα-binding metabolites were evident (Fig. 5D).

Identification of Tamoxifen and Raloxifene Metabolites. In Fig. 6, a provisional scheme of the metabolism of TAM by CYP enzymes is presented. Not all TAM metabolites, detected by UV and the ERα-affinity assay, were detected by LC–ESI–MS. The minor metabolites TM1 to TM4, TM6 and TM7 were all visible on the ERα-affinity traces, but could not be detected with LC-MS. Masses of the protonated molecules of metabolites TM5, TM8 to TM21 were subsequently determined by LC-MS (Table 2). Structural properties of the TAM metabolites formed based on CID mass spectra are discussed in the next section. The ERα-binding metabolite TM5 is a dihydroxylated secondary metabolite, as is indicated by the *m/z* value of 404. The *m/z* value of

374 for ERα-binding metabolites TM8, TM9 and TM10 indicates a secondary oxygenated N-desmethyl species. The ERα-binding metabolites TM11, TM12, TM14 and TM15 were identified as primary monohydroxy-TAM metabolites according to a protonated molecule with *m/z* 388. Based on *m/z* 358, TM13 was identified as a primary N-desmethyl-TAM metabolite which also showed significant binding to ERα. TM16 to TM19 were all identified as dihydroxy-TAM metabolites, which however did not show any traceable affinity in the ERα-affinity assay. The protonated molecule at *m/z* 374 for TM20 was assigned to an oxygenated N-desmethyl metabolite. According to the protonated molecule mass of 402, TM21 was a quinone. In Fig.7 the metabolic scheme of the metabolism of RAL by rat LM is depicted. We were able to measure protonated molecule masses from six ERα-binding and one non-ERα-binding metabolite of RAL. The first three metabolites eluting (RM1-RM3), are all dihydroxy-RAL species according the protonated molecules at *m/z* 506. RM4 to RM6 at *m/z* 480 are primary, monohydroxylated RAL metabolites. The protonated molecule at *m/z* 472 implies that RM7 is probably one of the two quinones recently described in literature (Yu *et al*., 2004).

DISCUSSION

Our primary aim was the development of a hyphenated and automated HRS system that can provide information of time-dependent formation and ERα-affinity of CYP-generated metabolites of SERMs. The CYP-bioreactor on-line coupled to SPE-HPLC enabled us to generate and swiftly trap and separate a substantial amount of CYP generated metabolites of both TAM and RAL. The metabolites were trapped very efficiently on SPE columns and isolated from air and light, they stayed protected from oxidation or UV-degradation. Additionally, because the incubation of the drugs took place prior to HPLC runs, microsomes were directly used which reduced degradation of CYP enzymes to a minimum. CYP enzymes are known to degrade to some extent, even when stored on ice (Yamazaki *et al*., 1997). For the detection of ERα-binding metabolites we made use of a previously developed and optimized on-line HRS ERα-affinity assay. Displacement of coumestrol from the ERα ligand binding domain results in a decreased fluorescence intensity of coumestrol (Oosterkamp *et al*., 1996; Schobel *et al*., 2001). From the HPLC column eluting TAM and RAL metabolites with affinity for the ERα caused clear and reproducible negative peaks in the baseline of the bioaffinity trace (Fig. 3B and 4B). The peak height depends on the concentration of the eluting compound and its ERα-affinity. According to the upward trends in the ERα progress curves (Fig. 5A-C), TAM was time-dependently metabolized by pig liver microsomes in 15 ERα-binding metabolites (Fig 3B). The ERα-affinity detection system proved to be very sensitive according to the response signals of TM1 to TM4, TM6 and TM7 since these metabolites were only detected by their ERα-affinity response and not by UV. The high relative standard deviations of the ERα-affinity signals with these low and moderate ERα-binding metabolites can be explained by the fact that variations between ERα-

affinity signals tend to increase when the respective bioaffinity signals are decreasing (Fig. 5B and 5C). When bioaffinity signals approach the lowest level of detection, noise is obviously becoming a prominent factor, leading to increased standard deviations and as a consequence higher RSDs. Biotransformation of RAL in the CYP-bioreactor by rat liver microsomes resulted in the formation of six ERα-binding metabolites (RM1-RM6, Fig. 4B). Again, upward trends in the formation of ERα-binding metabolites were evident (Fig. 5D). Consequently, the present bioanalytical method is not only useful for the screening and identification of individual metabolites in mixtures, but also for measuring the time-dependent formation of CYP-generated ERα-binding metabolites of compounds like TAM and RAL.

Metabolic Profiling of Tamoxifen. Interpretation of the MS-MS spectra of the metabolites was performed using the profile group concept proposed by Kerns *et al* (Mayol *et al*., 1994). Of the 21 TAM metabolites observed, 5 were identified as primary metabolites (TM11 to TM15) (Table 2, Fig. 6). Leveling of ERα-affinity progress curves (Fig. 5) can be explained by primary metabolites reaching steady state conditions as they are further metabolized into secondary metabolites. The primary metabolite TM13 was identified as N-desmethyl-TAM which, in humans, is catalyzed by CYP3A4 (Desta *et al.*, 2004). On the basis of UV data (not shown) it appeared to be the most abundant metabolite of TAM. According to their MS-MS spectra TM11 and TM12 were monohydroxylated on the aromatic 3 or 4 position (Table 2, Fig. 6) which are known to be catalyzed in humans by CYP3A4 (3-position) or CYP2D6 (4-position) (Crewe *et al.*, 2002; Desta *et al*., 2004). TM11 and TM12 are the second most abundant metabolites according to UV data. Considering the high relative affinity of TM11 for ERα, this metabolite is likely to be 4-hydroxy-TAM since previous studies showed that this metabolite of TAM is 30 - 100 times more potent than TAM itself (Fura, 2006). The CID mass spectrum of TM14 did not provide

structural information. TM15 was identified as TAM-N-oxide by its MS–MS spectrum (Table 2, Fig. 6) and is mainly formed by flavin-containing monooxygenases (FMOs) (Mani *et al*., 1993). The abundance of this metabolite was comparable to TM12, however, its ERα-affinity was very low (Fig. 3 and 5). The decreasing slope of its ERα-affinity progress curve can be explained by reduction of the N-oxide by CYP enzymes which is in line with the suggestion that N-oxide-TAM is a storage form of TAM *in vivo* (Mani *et al*., 1993).

Several primary metabolites of TAM are further metabolized into the secondary metabolites TM5, TM8 to TM10 and TM16 to TM21. The MS–MS spectrum of the dihydroxylated metabolite TM5 revealed hydroxylation in the a-ring and b-ring of TAM (Table 2, Fig. 6A), respectively yielding 4 (or 3), 4' (or 3')-dihydroxy-TAM. TM5 probably originates from TM11/TM12and is catalyzed in humans by CYP3A (Desta *et al.*, 2004). The MS–MS spectra of the oxygenated N-desmethyl metabolites TM8 and TM10 point to hydroxylation either in the a-ring of TAM (3 or 4 position) or on the alpha position of the ethylene moiety. Since the amount of TM8 formed is 150 times as low as TAM while its relative ERα-affinity is high, this metabolite is most likely endoxifen which is known to be as potent as 4-hydroxy-TAM (Johnson *et al*., 2004). The MS-MS spectrum of TM9 did not provide additional structural information. The CID spectrum of the dihydroxylated metabolite TM17 suggested that besides the ethyl moiety, the c-ring or ether linkage (e) in TAM is also hydroxylated, which is an observation hitherto not described. CID spectra of the dihydroxylated metabolites TM16, TM18 and TM20 did not reveal the positions of the hydroxyl group introduced. For the dihydroxylated metabolite TM19 we could identify hydroxylation of the ethyl moiety (d). The MS-MS spectrum of TM21 suggested that this metabolite is a diquinone of TAM, species also known to be produced by CYPs (Fan and Bolton, 2001). Finally, he fast elution times of the ERα-binding metabolites at

the beginning of the chromatogram (TM1-TM4) indicate that these are most likely tertiary metabolites. Introduction of additional hydroxyl groups or cleavage of methyl groups increase polarity and therefore shorten retention times in reversed phase chromatography.

In order to unambiguously substantiate the suggested structures of TAM metabolites, additional experiments should be carried out. For example standards of the suggested metabolites should be synthesized and their retention times and MS-MS spectra could be compared to those obtained with the present bioanalytical system. Furthermore, preparative HPLC and subsequent NMR analysis of the metabolites could provide more definite structural information.

Metabolic Profiling of Raloxifene. The metabolic profile of RAL is less complex than that of TAM. Only four primary and three secondary metabolites were observed when incubated with rat liver microsomes (Fig. 7). Formation of several ERα-binding metabolites showed clear upward trends according to Fig. 5D. Interpretation of the MS–MS spectra of the monohydroxylated RAL metabolites RM4 and RM5 lead to the conclusion that hydroxyl groups were introduced in either the a or b-ring of RAL as expected upon biotransformation by CYPs (Lim *et al*., 1999) (Table 3, Fig. 7). The fragments at *m/z* 405 and 269 suggest that RM6 is hydroxylated on the aromatic c-ring. This metabolite has not yet been described previously, despite the fact that CYPs are very well capable of hydroxylating aromatic moieties. MS–MS spectra of the dihydroxy-RAL species RM2 and RM3 provided also structural information. For RM2, fragments at *m/z* 363 and 269 point to hydroxylation in the piperidinic d-ring (Fig. 7) and aromatic c-ring. The *m/z* 389, 269 and especially *m/z* 144 fragments of RM3 strongly indicate that the d-ring is dihydroxylated. Both RM2 and RM3 have not yet been described in literature. The ion at *m/z* 472 implies that RM7 is likely one of the two quinine-metabolites recently described in literature (Yu *et al.*, 2004). Interestingly, except for the diquinone, all observed metabolites show significant ERα-affinity,

which may have consequences for the in vivo effect of RAL. Additional experiments should be performed in order to find definite proof.

Conclusion. We developed a fully automated on-line bioanalytical system for the metabolic profiling of SERMs. This system is based on the hyphenation of a gradient SPE-HPLC, a CYP-containing bioreactor and an on-line, HRS ERα-affinity assay. The system was validated with the two clinically used SERMs as model compounds, namely tamoxifen and raloxifen. The present bioanalytical method was able to provide simultaneously information about the time-dependent formation as well as about the ERα-affinity of CYP generated metabolites of TAM and RAL. For TAM we were able to identify 15 ERα-binding metabolites and 6 non-ERα-binding metabolites varying from trace amounts of tertiary metabolites to major primary ones. Amongst the ERα-binding metabolites we identified 4-hydroxy-TAM, N-oxide-TAM, N-desmethyl-TAM and the recently characterized, very potent endoxifen. We also could identify potentially carcinogenic α-hydroxy-TAM species. By analyzing RAL with the presented sytem, we were able to identify 6 ERα-binding metabolites of which three novel ones and one non-binding metabolite. These RAL metabolites include species that are hydroxylated on the piperidine ring. Overall, biotransformation of the SERMs analyzed, yields a very complex profile of ERα-binding and non-ERα-binding metabolites which might have considerable consequences for the pharmacological properties of these drugs. The hyphenated and fully automated bioanalytical system presented here, could be very useful for elucidation of convoluted metabolic profiles, and by inference become a novel tool in active metabolite screening e.g. for the purpose of drug discovery and development and for safety assessment research.

ACKNOWLEDGEMENTS

The PEEK filter unit, used to contain the PES filter, was made by D. J. van Ieperen and R. Boegschoten at the fine mechanical workshop of the Vrije Universiteit Amsterdam. The separate parts of the SPE-HPLC coupled bioreactor and HRS ERα-affinity detector were kindly provided by Kiadis B.V. (Groningen, The Netherlands). The ER LBD expressing E-coli cells were a kind gift of Dr. Marc Ruff and Dr. Dino Moras.

REFERENCES

Ali S and Coombes RC (2000) Estrogen receptor alpha in human breast cancer: occurrence and significance. *J Mammary Gland Biol Neoplasia* **5:**271-281.

Chen Q, Ngui JS, Doss GA, Wang RW, Cai X, DiNinno FP, Blizzard TA, Hammond ML, Stearns RA, Evans DC, Baillie TA and Tang W (2002) Cytochrome P450 3A4-mediated bioactivation of raloxifene: irreversible enzyme inhibition and thiol adduct formation. *Chem Res Toxicol* **15:**907-914.

Crewe HK, Notley LM, Wunsch RM, Lennard MS and Gillam EM (2002) Metabolism of tamoxifen by recombinant human cytochrome P450 enzymes: formation of the 4-hydroxy, 4'-hydroxy and N-desmethyl metabolites and isomerization of trans-4-hydroxytamoxifen. *Drug Metab Dispos* **30:**869-874.

Desta Z, Ward BA, Soukhova NV and Flockhart DA (2004) Comprehensive evaluation of tamoxifen sequential biotransformation by the human cytochrome P450 system in vitro: prominent roles for CYP3A and CYP2D6. *J Pharmacol Exp Ther* **310:**1062-1075.

Eiler S, Gangloff M, Duclaud S, Moras D and Ruff M (2001) Overexpression, purification, and crystal structure of native ER alpha LBD. *Protein Expr Purif* **22:**165-173.

Evans WE and Relling MV (1999) Pharmacogenomics: translating functional genomics into rational therapeutics. *Science* **286:**487-491.

Fan PW and Bolton JL (2001) Bioactivation of tamoxifen to metabolite E quinone methide: reaction with glutathione and DNA. *Drug Metab Dispos* **29:**891-896.

Fura A (2006) Role of pharmacologically active metabolites in drug discovery and development. *Drug Discov Today* **11:**133-142.

Gokhale MS, Bunton TE, Zurlo J and Yager JD (1997) Cytochrome P450 isoenzyme activities in cultured rat and mouse liver slices. *Xenobiotica* **27:**341-355.

Ingelman-Sundberg M and Rodriguez-Antona C (2005) Pharmacogenetics of drug-metabolizing enzymes: implications for a safer and more effective drug therapy. *Philos Trans R Soc Lond B Biol Sci* **360:**1563-1570.

Johnson MD, Zuo H, Lee KH, Trebley JP, Rae JM, Weatherman RV, Desta Z, Flockhart DA and Skaar TC (2004) Pharmacological characterization of 4-hydroxy-N-desmethyl tamoxifen, a novel active metabolite of tamoxifen. *Breast Cancer Res Treat* **85:**151-159.

Kool J, Ramautar R, van Liempd SM, Beckman J, de Kanter FJ, Meerman JH, Schenk T, Irth H, Commandeur JN and Vermeulen NP (2006) Rapid On-line Profiling of Estrogen Receptor Binding Metabolites of Tamoxifen. *J Med Chem* **49:**3287-3292.

Kool J, van Liempd SM, Ramautar R, Schenk T, Meerman JH, Irth H, Commandeur JN and Vermeulen NP (2005) Development of a novel cytochrome p450 bioaffinity detection system coupled online to gradient reversed-phase high-performance liquid chromatography. *J Biomol Screen* **10:**427-436.

Lim HK, Stellingweif S, Sisenwine S and Chan KW (1999) Rapid drug metabolite profiling using fast liquid chromatography, automated multiple-stage mass spectrometry and receptor-binding. *J Chromatogr A* **831:**227-241.

Mani C, Hodgson E and Kupfer D (1993) Metabolism of the antimammary cancer antiestrogenic agent tamoxifen. II. Flavin-containing monooxygenase-mediated N-oxidation. *Drug Metab Dispos* **21:**657-661.

Martino S, Cauley JA, Barrett-Connor E, Powles TJ, Mershon J, Disch D, Secrest RJ and Cummings SR (2004) Continuing outcomes relevant to Evista: breast cancer incidence in

postmenopausal osteoporotic women in a randomized trial of raloxifene. *J Natl Cancer Inst* **96:**1751-1761.

Mayol RF, Cole CA, Luke GM, Colson KL and Kerns EH (1994) Characterization of the metabolites of the antidepressant drug nefazodone in human urine and plasma. *Drug Metab Dispos* **22:**304-311.

Morello KC, Wurz GT and DeGregorio MW (2002) SERMs: current status and future trends. *Crit Rev Oncol Hematol* **43:**63-76.

Notley LM, De Wolf CJ, Wunsch RM, Lancaster RG and Gillam EM (2002) Bioactivation of tamoxifen by recombinant human cytochrome p450 enzymes. *Chem Res Toxicol* **15:**614-622.

Omura T and Sato R (1964) The Carbon Monoxide-Binding Pigment of Liver Microsomes. Ii. Solubilization, Purification, and Properties. *J Biol Chem* **239:**2379-2385.

Oosterkamp AJ, Villaverde Herraiz MT, Irth H, Tjaden UR and van der Greef J (1996) Reversed-phase liquid chromatography coupled on-line to receptor affinity detection based on the human estrogen receptor. *Anal Chem* **68:**1201-1206.

O'Regan RM and Jordan VC (2002) The evolution of tamoxifen therapy in breast cancer: selective oestrogen-receptor modulators and downregulators. *Lancet Oncol* **3:**207-214.

Roy U, Joshua R, Stark RL and Balazy M (2005) Cytochrome P450/NADPH-dependent biosynthesis of 5,6-trans-epoxyeicosatrienoic acid from 5,6-trans-arachidonic acid. *Biochem J* **390:**719-727.

Schenk T, Breel GJ, Koevoets P, van den Berg S, Hogenboom AC, Irth H, Tjaden UR and van der Greef J (2003) Screening of natural products extracts for the presence of phosphodiesterase inhibitors using liquid chromatography coupled online to parallel biochemical detection and chemical characterization. *J Biomol Screen* **8:**421-429.

Schobel U, Frenay M, van Elswijk DA, McAndrews JM, Long KR, Olson LM, Bobzin SC and Irth H (2001) High resolution screening of plant natural product extracts for estrogen receptor alpha and beta binding activity using an online HPLC-MS biochemical detection system. *J Biomol Screen* **6:**291-303.

Sharma M, Shubert DE, Lewis J, McGarrigle BP, Bofinger DP and Olson JR (2003) Biotransformation of tamoxifen in a human endometrial explant culture model. *Chem Biol Interact* **146:**237-249.

Spelsberg TC, Subramaniam M, Riggs BL and Khosla S (1999) The actions and interactions of sex steroids and growth factors/cytokines on the skeleton. *Mol Endocrinol* **13:**819-828.

van Liempd SM, Kool J, Reinen J, Schenk T, Meerman JH, Irth H and Vermeulen NP (2005) Development and validation of a microsomal online cytochrome P450 bioreactor coupled to solid-phase extraction and reversed-phase liquid chromatography. *J Chromatogr A* **1075:**205-212.

Yamazaki H, Inoue K, Turvy CG, Guengerich FP and Shimada T (1997) Effects of freezing, thawing, and storage of human liver samples on the microsomal contents and activities of cytochrome P450 enzymes. *Drug Metab Dispos* **25:**168-174.

Yenes S, Commandeur JN, Vermeulen NP and Messeguer A (2004) In vitro biotransformation of 3,4-dihydro-6-hydroxy-2,2-dimethyl-7-methoxy-1(2H)-benzopyran (CR-6), a potent lipid peroxidation inhibitor and nitric oxide scavenger, in rat liver microsomes. *Chem Res Toxicol* **17:**904-913.

Yu L, Liu H, Li W, Zhang F, Luckie C, van Breemen RB, Thatcher GR and Bolton JL (2004) Oxidation of raloxifene to quinoids: potential toxic pathways via a diquinone methide and o-quinones. *Chem Res Toxicol* **17:**879-888.

Zuber R, Anzenbacherova E and Anzenbacher P (2002) Cytochromes P450 and experimental models of drug metabolism. *J Cell Mol Med* **6:**189-198.

FOOTNOTES

The financial support for this project by Senter-Novem/BTS (#BTS00091) and Merck Research Laboratories (Drug Metabolism Department) is kindly acknowledged.

LEGENDS FOR FIGURES

Fig. 1) Schematic representation of the on-line bioreactor. P1: water pump; P2, P3: HPLC gradient pumps; P4: SPE wash pump;SV 1, 2, 5: 6-way dead-end switch valves; SV 3, 4: 2-position 6-port switch valves, closed lines indicate reaction mode and dotted lines wash mode; A.I.: autoinjector; SL: superloop 1 contained microsomes, SL 2 contained regenerating system, SL 3 contained 0.1% (v/v) AA and SL 4 contained 250 mM NaOH/0.5% (w/v) SDS; S: flow splitter (split ratio 1:8:1); bold lines originating from SV 1 are flow restrictors. After HPLC separation, eluted compounds are introduced in the bioassay (fig. 2).

Fig. 2) Schematic representation of the HRS ERα affinity assay. Compound, generated in the on-line bioreactor are introduced to the HPLC column. After separation, eluted compounds were screened separately on ERα affinity. P3, 4: HPLC gradient pumps; P5, 6: Make up gradient pumps; P7: water pump; SL: superloop 5: ERα solution, 6: coumestrol solution; S: flow splitters (split ratio 1:9); FLD: fluorescence detector.

Fig. 3) TIC chromatograms of mass ranges corresponding to tamoxifen metabolites with or without ERα-affinity (A). ERα affinity traces at increasing incubation time. From top to bottom the affinity traces correspond to 0, 7, 17 and 26 min incubation with Pig LMs (B). TIC chromatograms are correlated with ERα affinity traces of the on-line affinity assay.

Fig. 4) TIC chromatograms of mass ranges corresponding to raloxifene metabolites with or without ERα-affinity (A). ERα affinity traces at increasing incubation time. From top to bottom the affinity traces correspond to 0, 7, 17 and 26 min incubation with Rat LMs (B). TIC chromatograms are correlated with ERα affinity traces of the on-line affinity assay.

Fig. 5) Relative ERα-affinity progress curves where relative ERα-affinity is plotted against incubation time. Curves of highly active (A), moderately active (B) and slightly active metabolites (C) of TAM, generated by pig liver microsomes. Activity progress curves of RAL metabolites generated by PB-induced rat liver microsomes (D). Error bars represent 1 SD (n=3), data points at t=0 min represent incubations without regenerating system.

Fig. 6) Proposed metabolic scheme of the biotransformation of TAM by pig LM. The letters in the parent compound structure correspond to fragments of the molecule as seen in the tandem MS spectra (Table 2). The CYP subtypes indicated in the diagram correspond to the major contributing **human** isoforms.

Fig. 7) Proposed metabolic scheme of the biotransformation of RAL by rat LM. The letters in the parent compound structure correspond to fragments of the molecule as seen in the tandem MS spectra (Table 3). The CYP3A subtype in the diagram correspond to the **human** isoform.

TABLES

Table 1) Table of events in the on-line bioreactor.

Time (min)	Switch valve position					Events
	SV1	SV2	SV3	SV4	SV5	
0	b	a	a	a	e	Control (no RS)
2		b				Reaction } Injection and mixing of
4		c				Reaction substrates in reaction coil
6		d				Reaction
8	a	e	a	a	d	SPE conditioning
9	c	b				Coil emptying on SPE
13	e		b			Back flush filter and coil with water
14	d					Back flush filter and coil with NaOH/SDS
15	e					Back flush filter and coil with water
18	a	e	a		c	Start same procedure for respectively reaction coil ***c***, ***d***and ***a***
48	e	a	b	a	a	SPE wash (5% MeOH)
50				b		Beginning of gradient HPLC (70 min)
120				a	b	Start same procedure for respectively SPE column ***b***, ***c*** and ***d***

DMD Fast Forward. Published on June 21, 2006 as DOI: 10.1124/dmd.106.010355
This article has not been copyedited and formatted. The final version may differ from this version.

Table 2) Masses of tamoxifen metabolites with structural data obtained from MS/MS spectra.

Metabolites with traceable ERα-affinity			RT (min)	$[M+H]^+$ (*m/z*)	Δ (*m/z*)	MS/MS [a] (*m/z*)						
						-N	-N,-d	cde	abd	ad	other	
TAM	Tamoxifen		52.7	372	0	327	299	218	207	129		
TM 1			21.9	ND		ND						
TM 2			24.2	ND		ND						
TM 3			25.0	ND		ND						
TM 4			25.4	ND		ND						
TM 5	3 or 4-OH	3’ or 4’ -OH	28.0	404	+32	359	331		239	145	265	166
TM 6			29.2	ND		ND						
TM 7			32.0	ND		ND						
TM 8	N-desmethyl	3 or 4 or α-OH	35.1	374	+2	343			223	145	152	
TM 9	N-desmethyl	OH	37.9	374	+2	329			209		235	166
TM 10	N-desmethyl	3 or 4 or α-OH	38.4	374	+2	343			223	145	316	
TM 11	3 or 4 -OH		40.9	388	+16	343	315	234	223	145	166	
TM 12	3 or 4 -OH		43.6	388	+16	343	315		223	145	296	
TM 13	N-desmethyl		44.9	358	-14	327			207	129	152	
TM 14	-OH		48.1	388	+16	ND						
TM 15	N-oxide		49.5	388	+16	327	299		207		370	
Metabolites without traceable ERα-affinity												
TM 16	-OH	-OH	35.2	404	+32	ND						
TM 17	α-OH	c-ring-OH	40.3	404	+32	359	315		223	145	387	237
TM 18	-OH	-OH	42.4	404	+32	ND						
TM 19	α-OH	-OH	43.9	404	+32	358	315				386	199
TM 20	N-desmethyl	-OH	47.5	374	+2	ND						
TM 21	Quinone		55.5	402	+30						387	215

[a] Letters (a-e) correspond to those assigned to moieties in the structure of TAM in fig. 6a, N corresponds to the N-dimethyl group. Minus signs indicate the loss of the moiety in MS/MS.

DMD Fast Forward. Published on June 21, 2006 as DOI: 10.1124/dmd.106.010355
This article has not been copyedited and formatted. The final version may differ from this version.

Table 3) Masses of raloxifene metabolites with structural data obtained from MS/MS spectra.

Metabolites with traceable ERα-affinity			RT (min)	MS (*m/z*)	Δ (*m/z*)	MS/MS (*m/z*) -d	-e	ab	b	other		
RAL	Raloxifene		43.1	474		389	362	269	147	197		
RM 1	-OH	-OH	33.0	506	+32	ND						
RM 2	Piperidine-OH	c-ring-OH	34.7	506	+32			269		363	406	
RM 3	Piperidine-OH	Piperidine-OH	36.9	506	+32	389		269		470	144	
RM 4	OH in a or b-ring		38.9	490	+16	405	378	285				
RM 5	OH in a or b-ring		40.0	490	+16		378	285		472	418	269
RM 6	c-ring-OH		42.0	490	+16	405		269		472	389	
Metabolites without traceable ERα-affinity												
RM 7	Diquinone		52.0	472	-2		360	269		388		

[a] Letters correspond to those assigned to moieties in the structure of RAL in fig. 6b. The minus sign indicates the loss of the moiety in MS/MS.

1

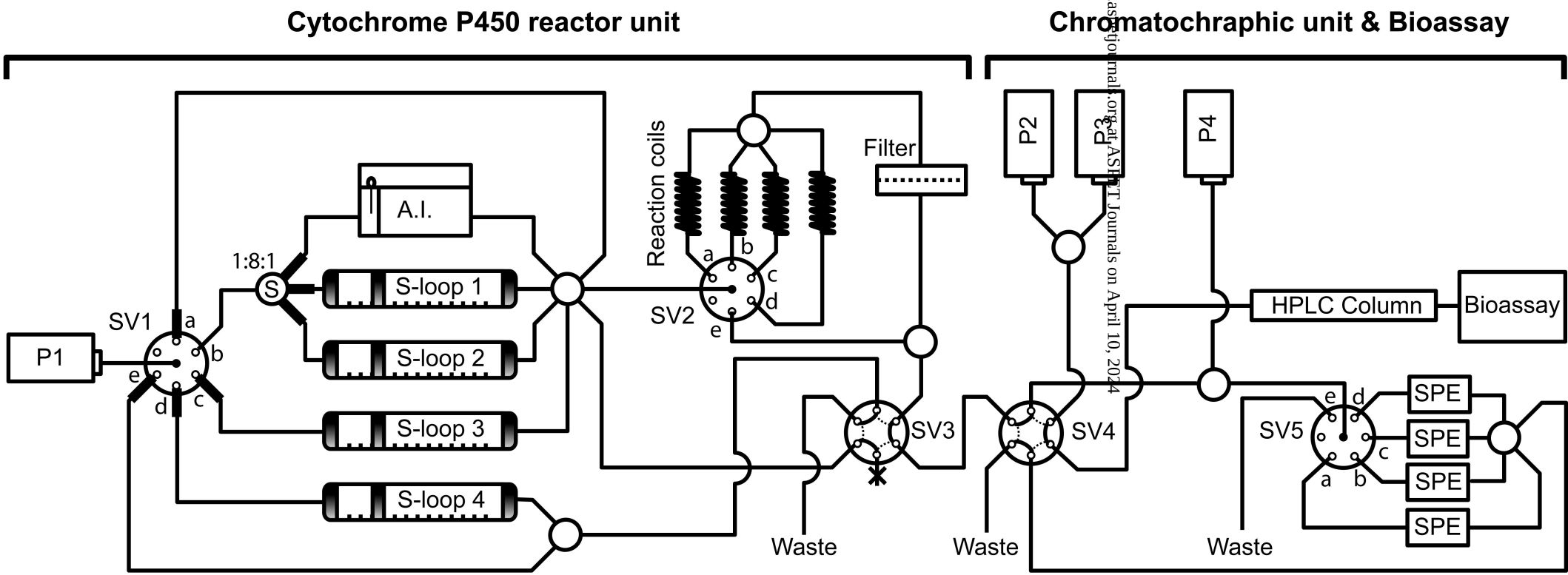

DMD Fast Forward. Published on June 21, 2006 as DOI: 10.1124/dmd.106.010355
This article has not been copyedited and formatted. The final version may differ from this version.

2

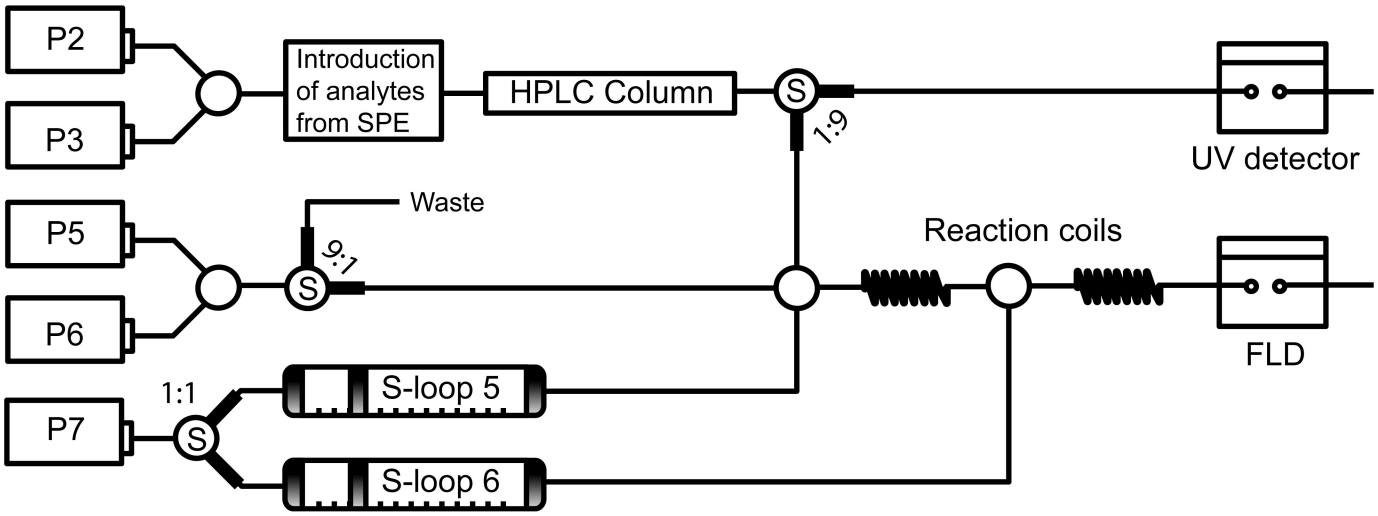

DMD Fast Forward. Published on June 21, 2006 as DOI: 10.1124/dmd.106.010355
This article has not been copyedited and formatted. The final version may differ from this version.

3

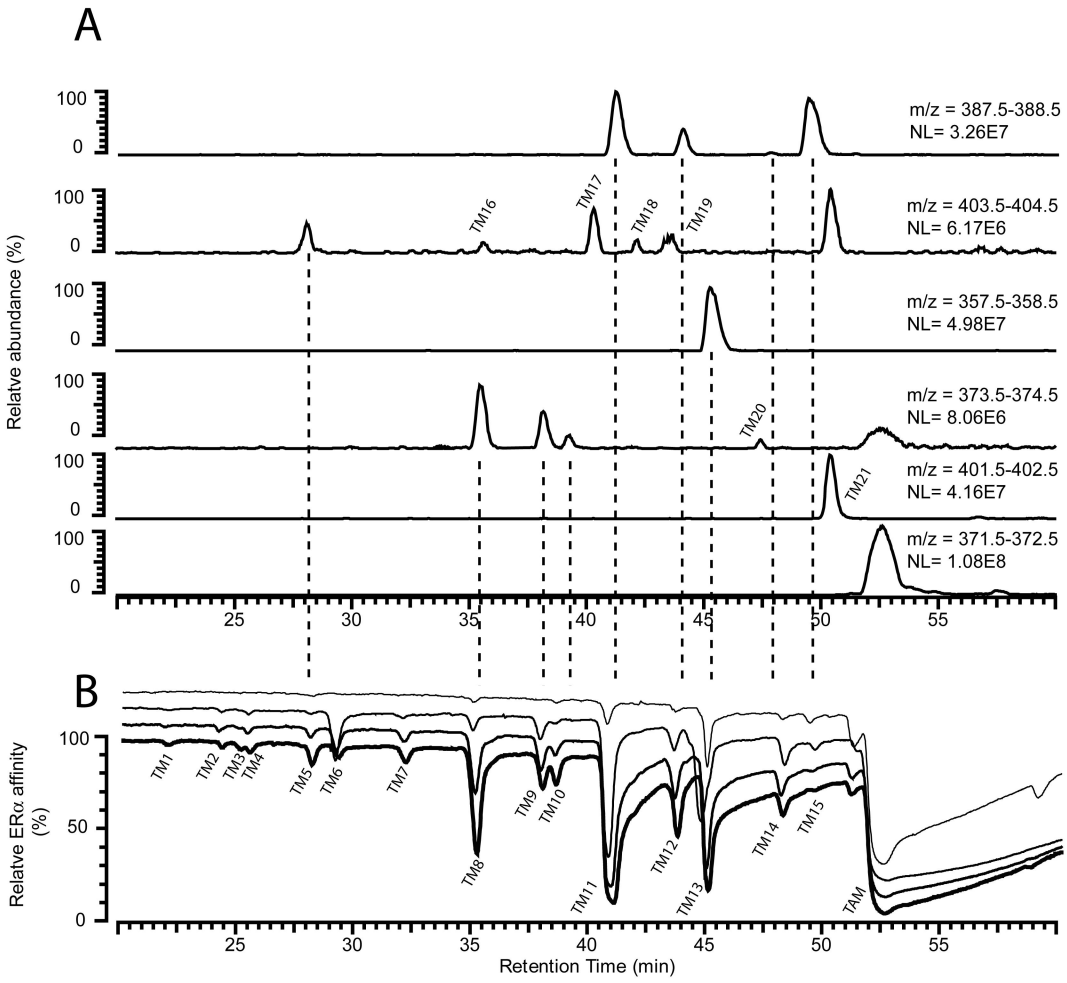

DMD Fast Forward. Published on June 21, 2006 as DOI: 10.1124/dmd.106.010355
This article has not been copyedited and formatted. The final version may differ from this version.

4

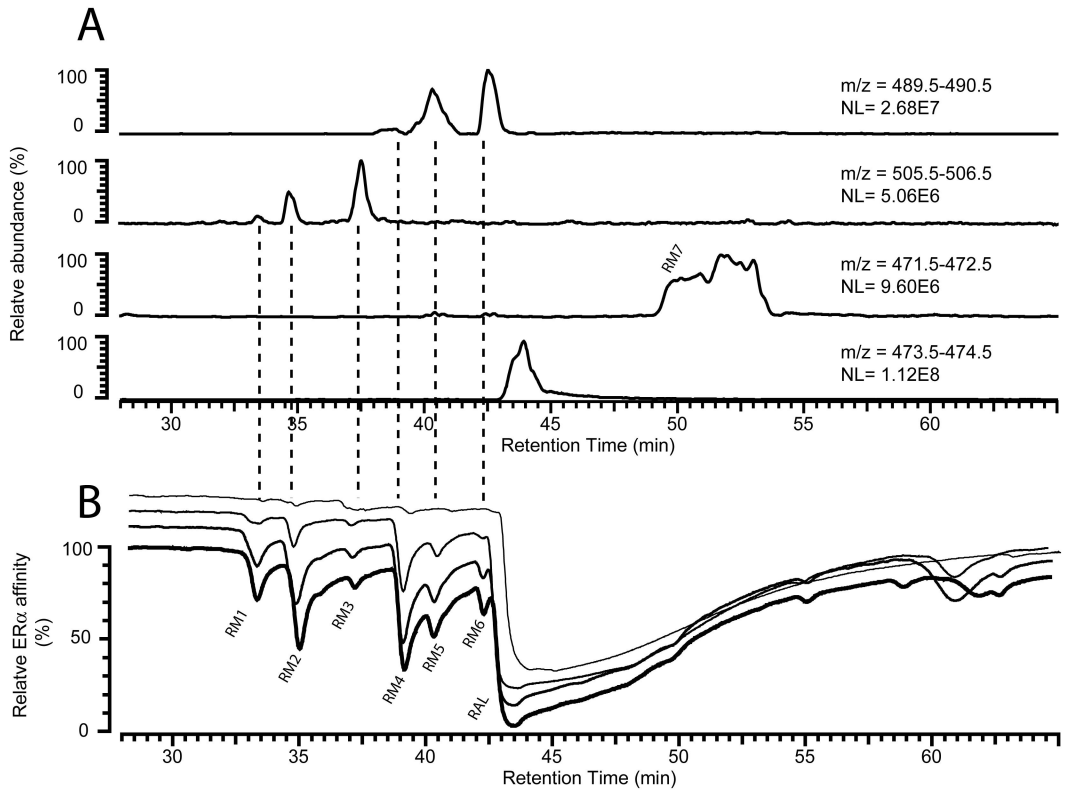

5

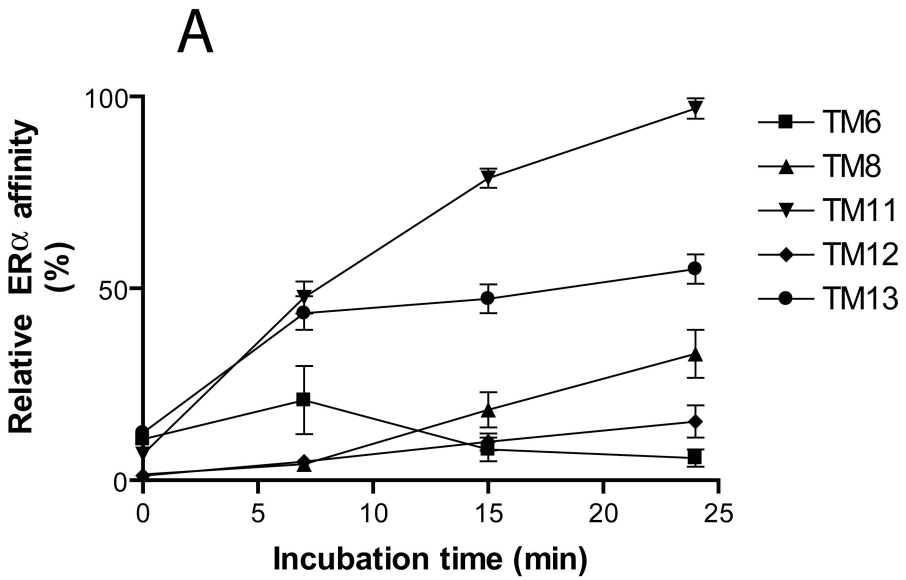

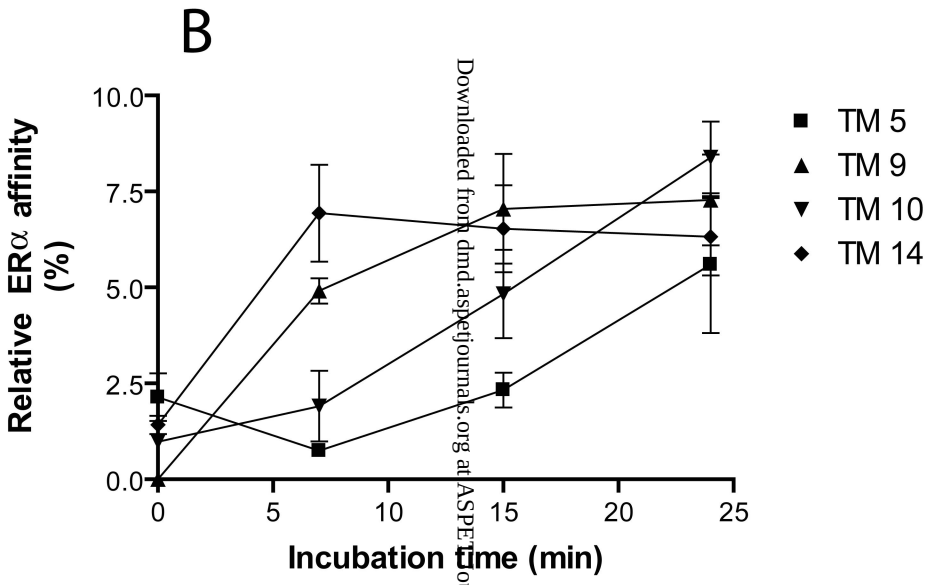

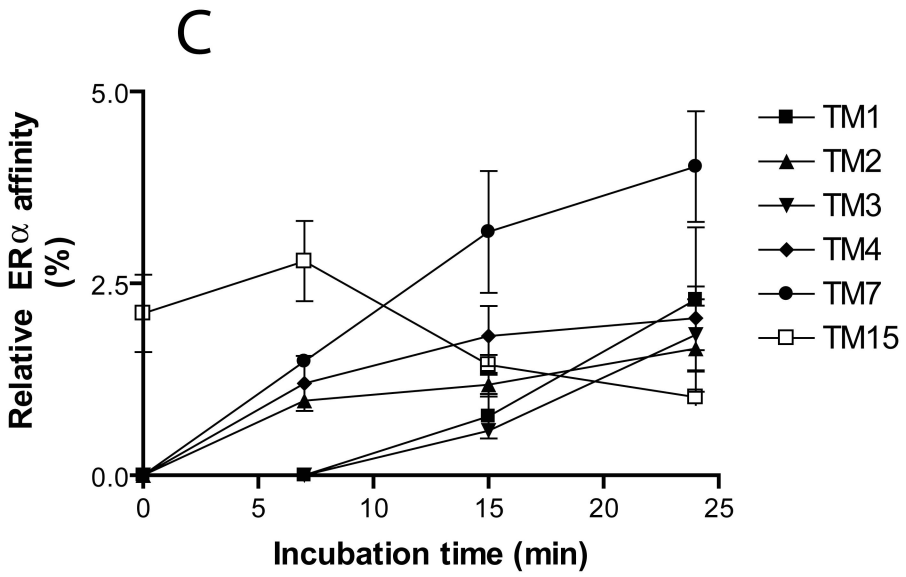

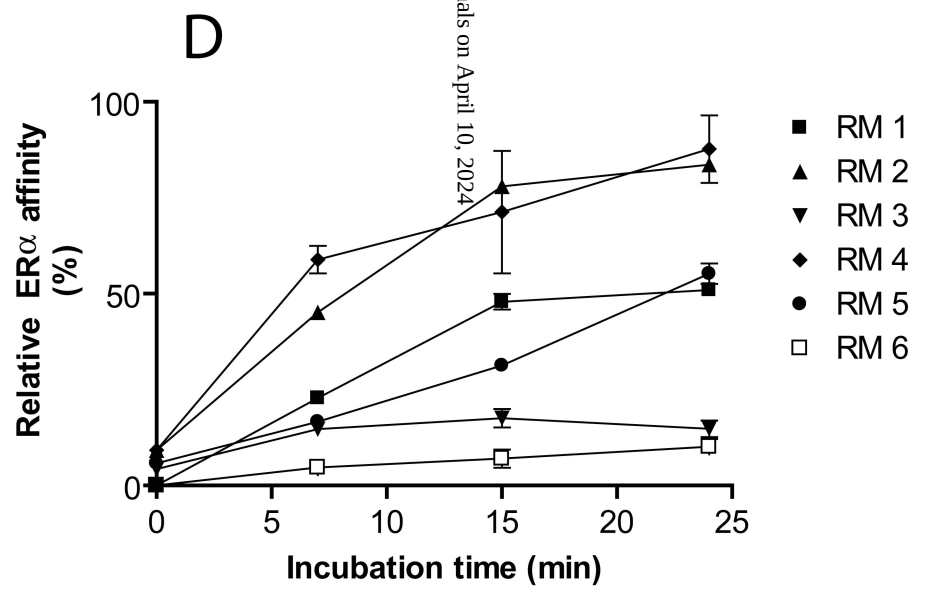

6

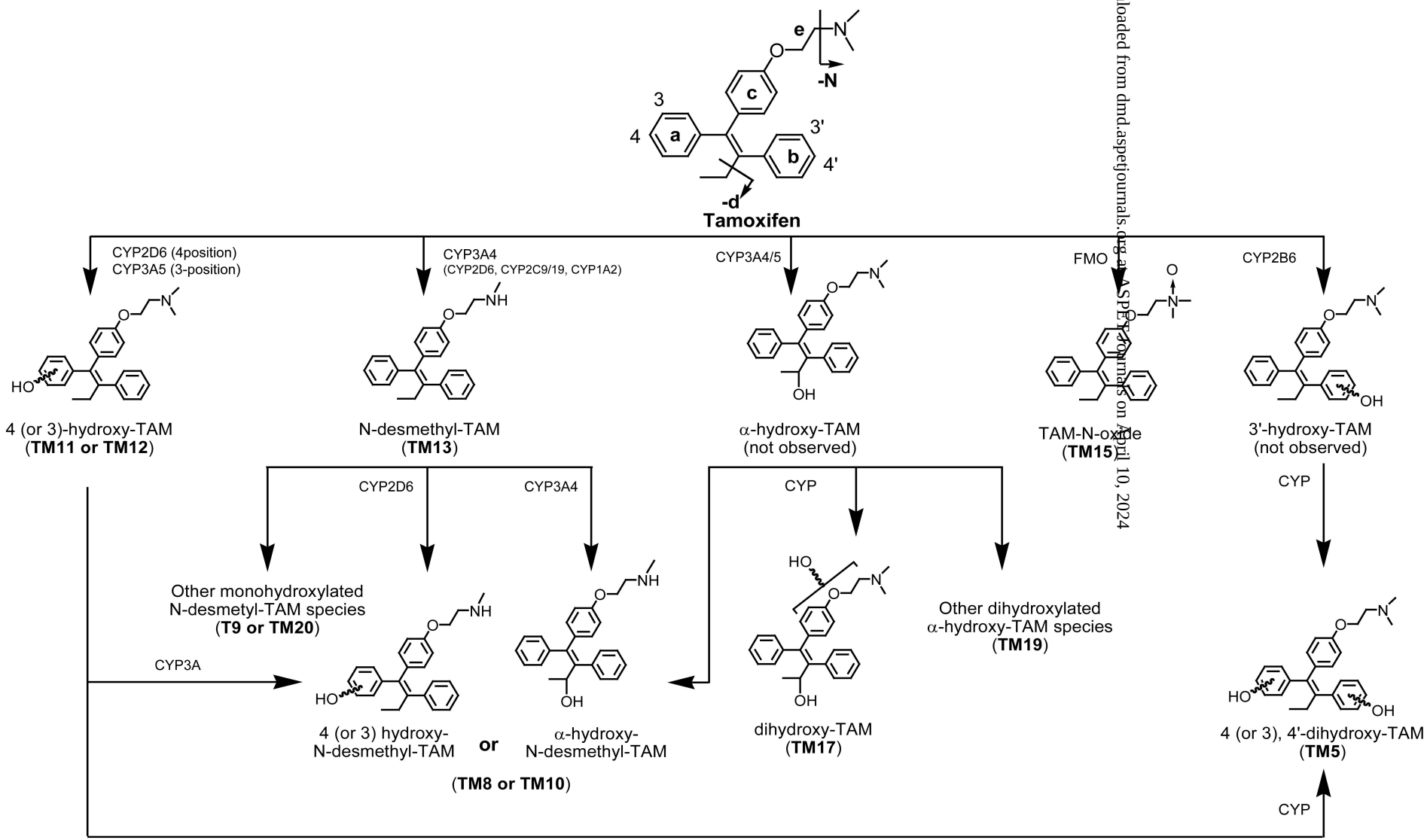

7